Electrostatic Control and Chloride Regulation of the Fast Gating of ClC-0 Chloride Channels

Tsung-Yu Chen, Mei-Fang Chen, and Chia-Wei Lin

Center for Neuroscience and Department of Neurology, University of California, Davis, CA 95616

ABSTRACT The opening and closing of chloride (Cl^-) channels in the ClC family are thought to tightly couple to ion permeation through the channel pore. In the prototype channel of the family, the ClC-0 channel from the *Torpedo* electric organ, the opening-closing of the pore in the millisecond time range known as "fast gating" is regulated by both external and internal Cl^- ions. Although the external Cl^- effect on the fast-gate opening has been extensively studied at a quantitative level, the internal Cl^- regulation remains to be characterized. In this study, we examine the internal Cl^- effects and the electrostatic controls of the fast-gating mechanism. While having little effect on the opening rate, raising $[Cl^-]_i$ reduces the closing rate (or increases the open time) of the fast gate, with an apparent affinity of >1 M, a value very different from the one observed in the external Cl^- regulation on the opening rate. Mutating charged residues in the pore also changes the fast-gating properties—the effects are more prominent on the closing rate than on the opening rate, a phenomenon similar to the effect of $[Cl^-]_i$ on the fast gating. Thus, the alteration of fast-gate closing by charge mutations may come from a combination of two effects: a direct electrostatic interaction between the manipulated charge and the negatively charged glutamate gate and a repulsive force on the gate mediated by the permeant ion. Likewise, the regulations of internal Cl^- on the fast gating may also be due to the competition of Cl^- with the glutamate gate as well as the overall more negative potential brought to the pore by the binding of Cl^-. In contrast, the opening rate of the fast gate is only minimally affected by manipulations of $[Cl^-]_i$ and charges in the inner pore region. The very different nature of external and internal Cl^- regulations on the fast gating thus may suggest that the opening and the closing of the fast gate are not microscopically reversible processes, but form a nonequilibrium cycle in the ClC-0 fast-gating mechanism.

KEY WORDS: ClC gating • electrostatic effect • foot-in-the-door

INTRODUCTION

ClC-0 from the electric organ of *Torpedo* rays (White and Miller, 1979; Jentsch et al., 1990; O'Neill et al., 1991) is the prototype of the ClC channel family, and its functional properties are the best known among all ClC members (for review see Jentsch et al., 1999, 2002; Maduke et al., 2000). This channel is a two-pore homodimer (Middleton et al., 1994, 1996; Ludewig et al., 1996; Lin and Chen, 2000), and the opening and closing of the channel pores are controlled by two functionally distinct gating mechanisms: the fast and the slow (inactivation) gating (Miller, 1982; Miller and White, 1984; Richard and Miller, 1990). The fast gating of ClC-0 controls each individual pore with kinetics in the millisecond range. On the other hand, the slow gating occurs in the time range of seconds, and this slower mechanism opens and closes the two pores simultaneously (for reviews see Miller and Richards, 1990; Maduke et al., 2000). These two gating mechanisms show an interesting feature: the gating appears to couple to the movement of Cl^- in the pore. Consequently, the gating properties are controlled by the Cl^- concentrations ($[Cl^-]$) in the extracellular and intracellular solutions (Richard and Miller, 1990; Pusch et al., 1995; Chen and Miller, 1996).

At the phenomenological level, changing both the external ($[Cl^-]_o$) and internal Cl^- concentrations ($[Cl^-]_i$) alters the fast-gating properties of the channel. External Cl^- is crucial in opening the fast gate. When $[Cl^-]_o$ is raised, the opening rate of the fast gate is increased, and this contributes to the apparent voltage dependence of the fast gating (Pusch et al., 1995; Chen and Miller, 1996). A kinetic model has been proposed to explain how the external Cl^- can open the fast gate in a depolarization-activated manner (Chen and Miller, 1996). Internal Cl^- also regulates the fast gating. The effect, however, is more prominent on the closing rate of the fast gate (Chen and Miller, 1996). It has been qualitatively described that when $[Cl^-]_i$ is elevated, the closing rate of the fast gate is reduced, a phenomenon very similar to the "foot-in-the-door" effect previously described in cation channels (Swenson and Armstrong, 1981).

Mei-Fang Chen's present address is Neuro-Medical Scientific Center, Tzu Chi General Hospital, 707, Sec.3, Chung-Yang Rd., Hualien 970, Taiwan.

Chia-Wei Lin's present address is Center for Research on Occupational and Environmental Toxicology, Oregon Health and Science University, Portland, OR 97201.

Address correspondence to Tsung-Yu Chen, Center for Neuroscience University of California-Davis, 1544 Newton Court, Davis, CA 95616. Fax: (530) 754-5036; email: tycchen@ucdavis.edu

J. Gen. Physiol. © The Rockefeller University Press • 0022-1295/2003/11/641/11 $8.00
Volume 122 November 2003 641–651
http://www.jgp.org/cgi/doi/10.1085/jgp.200308846

Understanding the control of the ClC-0 fast gating by Cl^- ions has been greatly facilitated by the recently solved high-resolution X-ray structures of the bacterial ClC channels (Dutzler et al., 2002, 2003). Fig. 1 shows a side-view of the inner pore region of the ClC channel with several residues likely lining the pore. The structures from bacterial ClC channels show that a glutamate residue, E148 (the residue in black on top of Fig. 1), which corresponds to E166 in ClC-0, projects its side chain into the ion permeation pathway. This glutamate side chain has been proposed to be the channel gate (Dutzler et al., 2002). In addition, three Cl^--binding sites were identified in the pore of mutant forms of the channel, in which E148 is mutated to alanine (E148A) or glutamine (E148Q) (Dutzler et al., 2003). The first binding site is at the center of the pore (S_{cen}), and the bound Cl^- is stabilized by the dipoles of helices and the sidechain hydroxyl groups of the pore residues. A second Cl^--binding site is internal to S_{cen}, and is located at a position where the intracellular aqueous vestibule meets the selectivity filter (S_{int}). Finally, in the E148 mutants, a third anion (not depicted) is observed in place of the negative charge on the E148 side chain in the wild-type (WT) channel. This Cl^--binding site, which is named S_{ext}, is only 4 Å external to S_{cen}. The presence of Cl^- at S_{ext} when the negative charge on the glutamate side chain is removed by mutation suggests a plausible mechanism for the gating-permeation coupling—a competition of Cl^- with the side chain of E166 (Dutzler et al., 2002, 2003).

The interpretation of Cl^- regulations of the fast gating based on the above competition model is complicated because external and internal Cl^- ions appear to have different effects on the fast gating. How would a single-gating mechanism be responsible for the two apparently different regulations by the internal and external Cl^- ions? In addition, a mutation far away from this glutamate gate at position K519 of ClC-0 is also known to change the fast-gating properties of this *Torpedo* channel (Pusch et al., 1995). K519 of ClC-0 is located at the intracellular pore entrance and is ~20 Å away from E166 based on the corresponding distance in the bacterial channel structure (Dutzler et al., 2002). If E166 is the fast gate, how could the mutation of K519 affect the fast gating? Even at the phenomenological level, it is not known if the mutation of K519 affects the opening rate, the closing rate, or both, since these two kinetic parameters can be differentially regulated by Cl^- ions coming into the pore from different directions.

The residue K519 of ClC-0 is important not only in the fast-gating mechanism but also in the control of channel conductance. We have recently shown that the charge on this residue contributes to the intrinsic electrostatic potential of the pore, which determines the conductance of the channel (Chen and Chen, 2003),

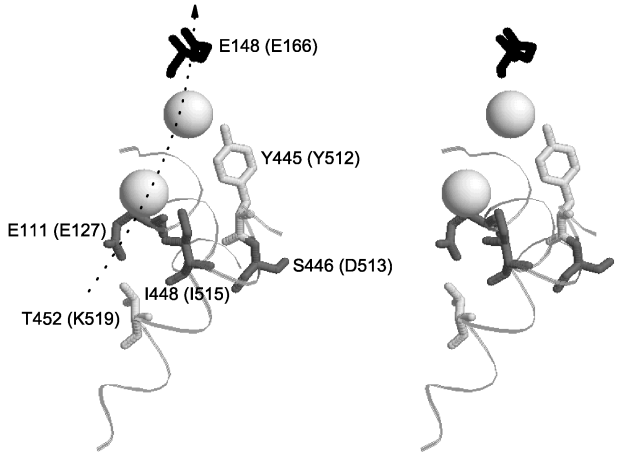

FIGURE 1. Stereo view of the inner pore region of the bacterial ClC channel. Extracellular side of the molecule is on top. The labeling outside and inside the parentheses represents residues of the bacterial and the *Torpedo* channel, respectively. The two spheres represent the two Cl^- ions at S_{cen} (top) and S_{int} (bottom). To reveal the relations of these residues with respect to the glutamate gate, E148 (E166 of ClC-0) is shown in black on top. The dotted, curved arrow roughly represents the ion permeation pathway. Ribbons represent helices D and R where these residues are located. Structural coordinates were taken from Protein Data Bank with the accessing code 1OTS.

and, in the case of pore cysteine mutants, controls the cysteine modification rate by charged methane thiosulfonate (MTS) reagents (Lin and Chen, 2003). In addition, we also showed that mutations of other residues lining the inner pore region change the ion flux across the pore. The positions of these residues, including E127, Y512, I515, and K519, and their relations to the proposed glutamate gate can be viewed from the stereo picture in Fig. 1. Since the gating of the channel is thought to be tightly linked to ion permeation, we suspect that the mutations of these pore-lining residues would also affect the fast gating of the channel via the permeant ions in the pore. In this study, we examine the effects of $[Cl^-]_i$ and the intrinsic electrostatic potential of the pore on the fast-gating to explore the mechanistic operation of ClC-0. We trace the path of a Cl^- ion and analyze the gating parameters from mutants that likely alter the Cl^- occupancy in the pore. The results reveal that internal Cl^- exerts an effect on the closing rate of the fast gate with a much lower apparent affinity than that of the external Cl^- effect on the opening rate. When the pore residues are made more positive by mutations, the opening and the closing rates of the fast gate are increased. On the other hand, when the intrinsic electrostatic potential of the pore is more negative, the fast gating is slower. Thus, the effect of $[Cl^-]_i$ on the fast-gate closing rate may come not only from a direct competition of Cl^- with the negatively charged glutamate side chain, as sug-

gested from the X-ray crystal structures of the bacterial ClC channel, but also from an overall more negative potential brought into the pore by Cl^- binding. Because the opening and the closing of the ClC-0 fast gate are controlled by external and internal Cl^- in a very different way, we also suggest that these two kinetic aspects of the fast gating likely are not the two opposite directions of a reversible gating process, but form a gating cycle during the operation of the ClC-0 fast gating.

MATERIALS AND METHODS

Mutagenesis and Channel Expression

Mutations at various positions were conducted by means of PCR mutagenesis as described in the previous paper (Chen and Chen, 2003). Most of the mutations were constructed in the background of the C212S mutation to remove the inactivation of the channel (Lin et al., 1999). Some of the mutants were also constructed in the WT background, and the difference in fast gating in the WT and C212S background is not significant. We therefore refer to the C212S mutant as the WT channel. All the channels examined were expressed in *Xenopus* oocytes, and RNA synthesis and oocyte preparation/injection were the same as those described previously (Chen, 1998; Lin et al., 1999).

Single-channel Recordings

Excised inside-out patch configuration (Hamill et al., 1981) was performed in all single-channel recordings. The recording pipettes were pulled from borosilicate glass capillaries by a pipette puller PP-830 (Narashige), and had resistance of 3–6 MΩ when filled with the pipette solution. In all experiments, the pipette (external) solution was the same and contained (in mM): 110 NMDG-Cl, 5 $MgCl_2$, 1 $CaCl_2$, 5 HEPES, pH 7.5. The standard bath (internal) solution in which high GΩ seals were made contained (in mM): 110 NaCl, 5 $MgCl_2$, 1 EGTA, 5 HEPES, pH 7.5. Various internal solutions containing 30–2,400 mM $[Cl^-]_i$ have a content of (in mM): (X-10) NaCl, 5 $MgCl_2$, 1 EGTA, 5 HEPES, pH 7.5, where X represents the indicated $[Cl^-]_i$. For solutions containing $[Cl^-]_i$ <120 mM (such as 30 or 60 mM), Na-glutamate was added to make the ionic strength similar to the 120 mM Cl^- solution. The pH's of the internal and external solutions were adjusted with NaOH and NMDG, respectively. For most single-channel recordings, the current was online filtered at 0.2 kHz (−3 dB), and digitized at 1 kHz. In analysis the current was further digitally filtered at 0.2 kHz, leading to a final cut-off frequency at ∼140 Hz. For mutants with fast kinetics (such as I515K and D513S, see Fig. 7), the filter frequency and the sampling rate were 0.5 and 2.5 kHz respectively. The exchange of internal solution was achieved using a SF-77 solution exchange system (Warner Instruments, Inc.) as described previously (Chen and Chen, 2003). The presented voltages in the current study were not corrected for junction potentials.

Data Analysis

Because some mutants were constructed in the WT background, the inactivation events of the channel were sometimes difficult to separate from the closed events. For all the results presented, the analysis of the single-channel traces, which comprise three equidistant current levels, was made according to the method described previously (Chen and Miller, 1996; Chen and Chen 2001). This analysis method exploits the fact that the ratio of the state-probabilities for the fully-open and the middle-current level (f_2/f_1) as well as the dwell-time of the events at these two current levels (τ_2 and τ_1, respectively) are completely independent of the inactivation time. Thus, under the assumption that the channel contains two pores independently controlled by their fast gates (Miller, 1982; Hanke and Miller, 1983; Miller and White, 1984; Bauer et al., 1991; Middleton et al., 1996; Ludewig et al., 1996; Lin and Chen, 2000), the overall open probability (P_o) of the fast gate is determined from eq. 1:

$$P_o = 2\sigma/(1+2\sigma), \tag{1}$$

where $\sigma = f_2/f_1$. The opening rate (α) and the closing rate (β) are calculated according to Eqs. 2a and b:

$$\alpha = P_o/\tau_1 \tag{2a}$$

$$\beta = (1-P_o)/\tau_1. \tag{2b}$$

To show the saturation effect on the fast gating of the channel by increasing $[Cl^-]_i$, we plotted the averaged open duration of an individual pore (τ_o) as a function of internal Cl^- activity. For comparison, the averaged duration of the closed events (τ_c) was also estimated from the opening rate. The estimate of τ_o and τ_c was based on Eqs. 3a and b:

$$\tau_0 = 1/(2\beta) \tag{3a}$$

$$\tau_c = 1/(2\alpha). \tag{3b}$$

The dependence of the open duration of the fast gate on the internal Cl^- activity is fitted by an empirical hyperbolic equation:

$$\tau_0 = \tau_{min} + (\tau_{max} - \tau_{min})A_{Cl}/(A_{Cl} + K_{1/2}), \tag{4}$$

where τ_{min} and τ_{max} are the open duration of the channel at zero and infinite internal Cl^- activity, respectively, A_{Cl} is the internal Cl^- activity, and $K_{1/2}$ is the Cl^- activity at which the half maximal effect on the open duration was observed. The calculation of the internal Cl^- activity was based on the equation $A_{Cl} = \mu[Cl^-]$, using the following activity coefficients (μ): 30 mM, 0.930; 60 mM, 0.867; 120 mM, 0.769; 300 mM, 0.710; 600 mM, 0.673; 1,200 mM, 0.654; 2,400 mM, 0.684 (Robinson and Stokes, 1955). Throughout the whole paper, the averaged data were expressed as mean ± SEM. Curve fitting was performed with an un-weighted, least-squares method using Origin software (OriginLab Co.).

RESULTS

The internal Cl^- effects on fast gating have been previously described at a qualitative level. Increasing $[Cl^-]_i$ significantly reduced the fast-gate closing rate but had only a minor effect on the opening rate (Chen and Miller, 1996). To quantitatively characterize the internal Cl^- effect, we recorded single ClC-0 channels with the excised inside-out configuration, and systematically varied $[Cl^-]_i$ from 30–2,400 mM. Fig. 2 A shows the representative single-channel recording traces of the WT channels and their analyses with dwell-time histograms of the three current levels. While raising $[Cl^-]_i$ from 120 to 2,400 mM has little effect on the durations of closed events (represented by open squares in the

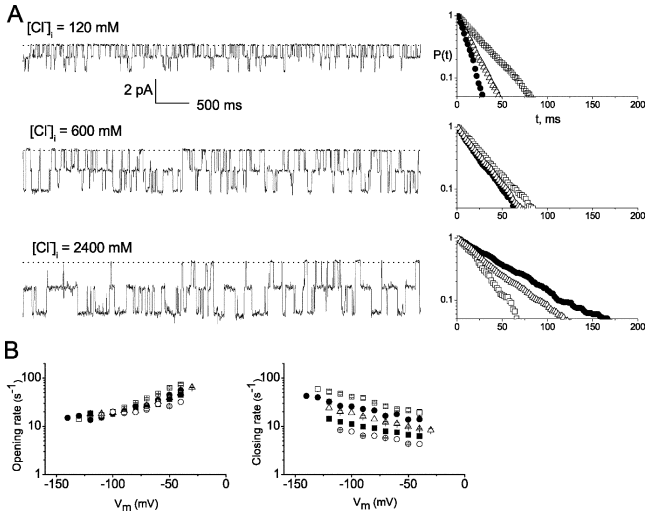

FIGURE 2. Gating effects of $[Cl^-]_i$ on the WT channel. (A) Single-channel recordings and dwell-time analyses of the WT channel. (Left) Recording traces at various $[Cl^-]_i$ as indicated. $V_m = -110$ mV, and $[Cl^-]_o = 120$ mM. (Right) Dwell-time histograms from continuous recordings containing the 6-s traces on the left. Symbols are: □, closed level; Δ, middle level; and ●, fully open level. The length of the analyzed trace and the number of events in each analysis at closed, middle, and fully open levels, respectively, are: (120 mM) 62 s and 1,147, 1,572, 426; (600 mM) 60 s and 659, 1,251, 593; (2,400 mM) 52 s and 197, 644, 449. (B) Averaged opening rate (left) and closing rate (right) of WT ClC-0 under different $[Cl^-]_i$. The rate parameters were calculated according to Eqs. 2a and b, and plotted (in logarithmic scale) as a function of the membrane potential V_m. Symbols for $[Cl^-]_i$ (in mM) are: □, 120; ●, 300; Δ, 600; ■, 1,200; ○, 2,400.

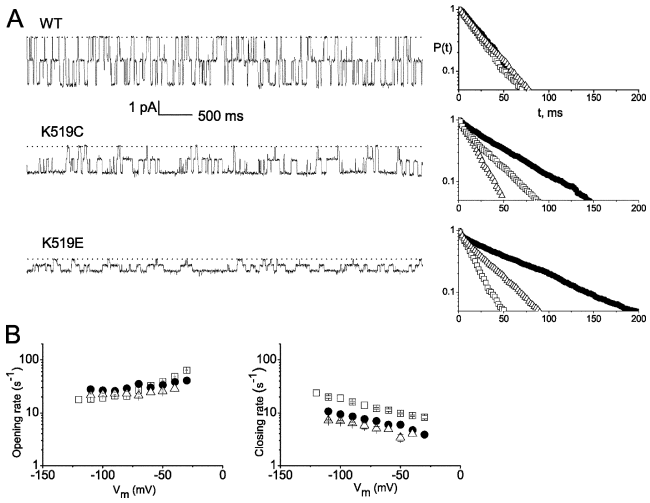

FIGURE 3. Mutational effects of residue K519 on the fast gating properties of ClC-0. (A) Single-channel recordings and dwell-time analyses for the WT channel and K519C and K519E mutants. $V_m = -110$ mV; $[Cl^-]_o = 120$ mM; $[Cl^-]_i = 600$ mM. Symbols in the dwell time histograms represent the same current levels as indicated in Fig. 2 A. The length of the analyzed trace and the numbers of events (closed, middle and fully open levels) for each analysis were: (WT), 50 s and 480, 1,010, 532; (K519C) 92 s and 457, 1,452, 997; (K519E) 112 s and 446, 1,561, 1,118. (B) Averaged opening and closing rates for the three channels shown in A as a function of voltage. Experimental conditions are as in A. Symbols are: □, WT; ●, K519C; Δ, K519E.

dwell-time histograms), the same increases in $[Cl^-]_i$ significantly prolong the durations of the fully open events (filled circles in the dwell-time histograms). As the durations of the closed and open events are inverse functions of the opening and closing rates, respectively (Eqs. 3a and b), the dwell-time histograms demonstrate that the major effect of $[Cl^-]_i$ is on the closing rate of the fast gate. Fig. 2 B shows the averaged opening and closing rates of the channel at various $[Cl^-]_i$ as a function of membrane voltage. Although an increase of $[Cl^-]_i$ appears to slightly reduce the opening rate at the depolarized potentials, the effect is very small (Fig. 2 B, left). On the other hand, increasing $[Cl^-]_i$ significantly reduces the closing rate so that the entire closing rate-voltage curve is shifted in parallel (Fig. 2 B, right). These results are consistent with those in the previous single-channel study using native ClC-0 channels directly purified from *Torpedo* electric organ (Chen and Miller, 1996).

In studying the external Cl^- regulation on the fast gating of ClC-0, Pusch et al. (1995) first drew attention to a basic residue K519 in ClC-0. By mutating this positively charged residue to glutamate (K519E), they showed that the fast gating of the channel was altered. However, since K519 was located on the intracellular side of the membrane, these authors could not conclude that K519 was directly involved in forming the anion binding site mediating the external Cl^- effect (Pusch et al., 1995). Thus, how the mutation of this residue affected the channel gating was not known. To investigate the functional role of K519 in the Cl^- regulation of fast gating, we compare the fast-gating kinetics among the WT (K519), K519C, and K519E channels at the single-channel level (Fig. 3). Representative single-channel traces and dwell-time histograms are shown in Fig. 3 A, and the averaged results of the opening and closing rates at $[Cl^-]_i = 600$ mM are plotted as a function of the membrane voltage in Fig. 3 B. It can be seen that mutation of K519, again, alters the closing rate much more than the opening rate. Furthermore, when the side chain charge of residue 519 is made more negative, the closing rate is reduced, and the closing rate-voltage curve is also shifted in parallel, a phenomenon similar to that of raising $[Cl^-]_i$. As for the WT channel, varying $[Cl^-]_i$ has little effect on the opening rate in the mutant channels. On the other hand, the closing rates of these channels are affected significantly by altering $[Cl^-]_i$ (see below). This "foot-in-the-door"-like effect (Swenson and Armstrong, 1981)—the higher the $[Cl^-]_i$, the longer the duration of the open events—can

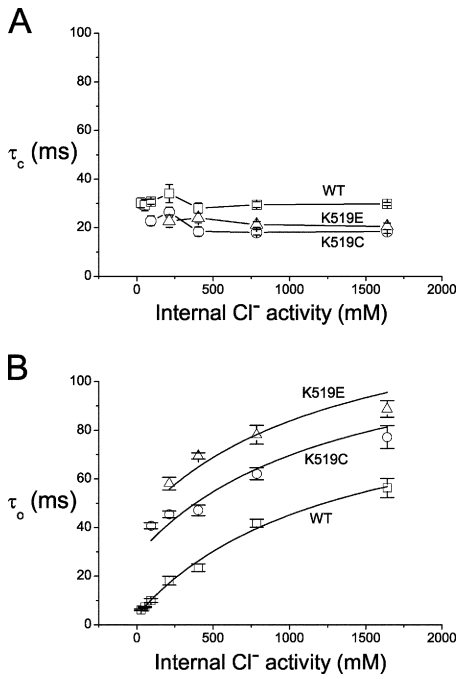

FIGURE 4. Dependence of the fast-gate closed (τ_c) and open durations (τ_o) on internal Cl^-. τ_o and τ_c were calculated according to Eqs. 3a and b, respectively. $V_m = -110$ mV. (A) τ_c as a function of internal Cl^- activity. Symbols are: squares, WT; circles, K519C; triangles, K519E. Data points are connected by straight lines. (B) τ_o as a function of internal Cl^- activity. Solid curves were drawn according to Eq. 4. The fitted parameters (τ_{min}, τ_{max}, and $K_{1/2}$) for the WT channel (squares) were: 3.8 ms, 95.5 ms, and 1,313 mM. In fitting the data points for K519C and K519E channels, the values of τ_{max}, and $K_{1/2}$ were fixed as those for the WT channel. The fitted values of τ_{min} in these two channels were 28.4 and 42.5 ms, respectively.

also be directly observed from previous published recording traces (see Fig. 4 of Chen and Chen, 2003).

To dissect out the effects of $[Cl^-]_i$ from those of the charge mutations, the closed durations (τ_c, reflecting the opening rate) and the open durations (τ_o, reflecting the closing rate) of the fast gate of these three channels are directly compared in Fig. 4, A and B, respectively. In this figure, we calculate τ_c and τ_o from the recording traces at -110 mV, and plot the data as a function of internal Cl^- activity. The values of τ_c for these three channels are similar to each other, ranging from ~15–35 ms, and raising $[Cl^-]_i$ from 30 to 2,400 mM (or A_{Cl} from 28 to 1642 mM) does not significantly change the value of τ_c (Fig. 4 A). On the other hand, a very similar pattern of the internal Cl^- effect on τ_o is observed for all three channels—the open duration increases with Cl^- activity, but the relation is not a straight line (Fig. 4 B). This result is consistent with the idea that the effect may be mediated through a Cl^--binding site. For the WT channel, fitting the data points to an empirical hyperbolic relation shows a half-saturating Cl^- activity of ~1,300 mM (Fig. 4 B), a value significantly higher than the $K_{1/2}$ in the Cl^- titration curve for the pore conductance (~60–75 mM, see White and Miller, 1981; Chen and Chen, 2003). It appears that there is a finite open duration of ~3–4 ms even in the absence of intracellular Cl^-. For the K519C and K519E mutants, the Cl^- titration curves are shifted in parallel toward longer open duration, and the more negative the charge at position 519, the longer is the open duration of the fast gate. Therefore the charge at position 519 controls the minimal open duration in the absence of internal Cl^- but appears to have less effect on the apparent affinity of the potential Cl^--binding site that is responsible for this effect.

Because the closing rate is affected by Cl^- ions and the charge mutation in the pore in a similar manner (Figs. 2 and 3), we ask if the alteration in the closing rate by Cl^- is a specific effect to the permeant ions. To this end, we examine if other anions, such as bromide (Br^-), a permeant ion, or sulfate (SO_4^{2-}), a nonpermeant ion, can exert similar gating effects. In these experiments, $[Cl^-]_i$ was constant in the intracellular solutions (300 mM in Br^- experiments and 120 mM in SO_4^{2-} experiments), and various concentrations of Br^- or SO_4^{2-} were added to the solutions. Fig. 5 A shows the single-channel conductance of the WT channel in the presence of various concentrations of internal Br^-. The conductance of the channel is reduced by Br^-, with an estimated apparent blocking affinity of ~24 mM (Fig. 5 A). Because Br^- can permeate through the pore (unpublished data), the half-blocking concentration here may not precisely reflect the true blocking affinity of Br^-. From the same experiments, the open durations of the fast gate are estimated and shown in Fig. 5 B. Similar to the internal Cl^- effect on the channel gating, an elevation of $[Br^-]_i$ increases the open duration of the fast gate. The titration curve for this Br^- effect is not linear, similar to the action of Cl^-. The effect of $[Br^-]_i$ on the open duration of the channel is stronger than that exerted by $[Cl^-]_i$ because at the same total concentration of the internal anions the open duration is longer in the presence of Br^-. On the other hand, the nonpermeant ion SO_4^{2-} does not have an appreciable effect on the open duration of the fast gate. In the presence of 120 mM $[Cl^-]_i$ with additional 180 or 480 mM SO_4^{2-}, the open duration is the same as that in the absence of this nonpermeant ion (Fig. 5 B).

The increase of the open duration (or the reduction of the closing rate) by the permeant ions Cl^- and Br^-, but not by the nonpermeant ion SO_4^{2-}, is consistent with the idea that the gating effects from Cl^- and Br^- occur in the pore. To examine if the effects of K519 mutations on the ClC-0 fast gating are also mediated by a pore mechanism, we explore the electrostatic control of the fast gating by manipulating the charge of pore

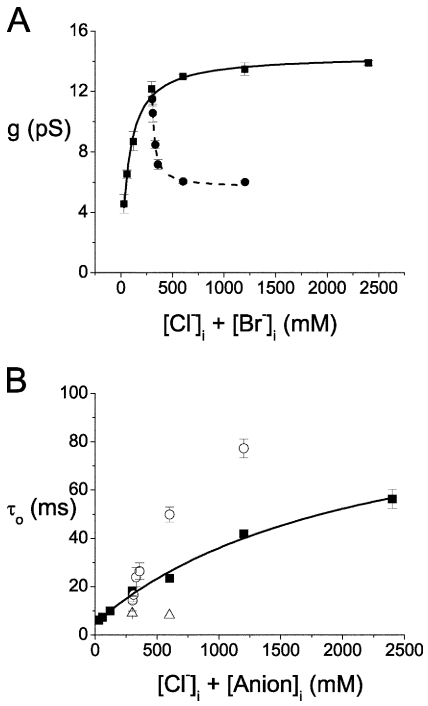

FIGURE 5. Effects of permeant and nonpermeant ions on the gating and permeation properties of WT ClC-0. (A) Blocking effects of Br^- on the conductance of the WT channel. Squares and the solid curve are the conductance-$[Cl^-]$ curve for the WT channel in the absence of Br^-. Circles are obtained in 300 mM $[Cl^-]_i$ plus 3, 10, 30, 60, 300, and 900 mM Br^-, respectively. Conductance in various ionic conditions was determined from the slope of the single-channel i-V curve (Chen and Chen, 2003). Dotted curve represents the best fit to an equation: $g = g_{min} + (g_{max} - g_{min})/(1+([Br^-]/K_{1/2})$, where g_{max} (=12.17 pS) is the conductance at $[Cl^-]_i$ = 300 mM in the absence of Br^-. The fitted g_{min} and $K_{1/2}$ were 5.6 pS and 23.8 mM, respectively. (B) Gating effects of Br^- and SO_4^{2-} on the WT channel. τ_o was estimated from the closing rate according to Eq. 3a. Solid squares and the solid curve were the same as those from the WT channel in Fig. 4 except the data were plotted against $[Cl^-]_i$. Open circles were from the Br^- experiments as those described in A. Open triangles were from recordings at 120 mM $[Cl^-]_i$ plus 180 and 480 mM SO_4^{2-}. All experiments shown in A and B were from recordings at the membrane potential of −110 mV.

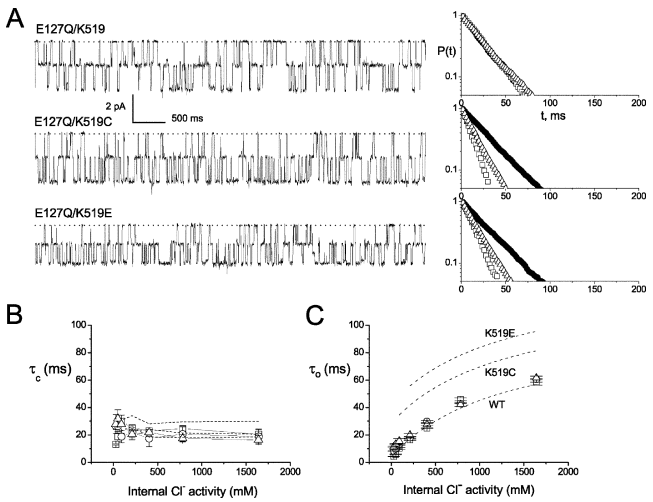

FIGURE 6. Functional role of E127 in the fast gating of ClC-0. (A) Single-channel recording traces and dwell-time histograms of E127Q/K519, E127Q/K519C, and E127Q/K519E. Symbols in the histograms represent the same current levels as those described in Fig. 2 A. V_m = −110 mV. $[Cl^-]_i$ = 600 mM. (B) Averaged closed durations of the three channels shown in A as a function of internal Cl^- activity. Symbols are: squares, E127Q/K519; circles, E127Q/K519C; triangles, E127Q/K519E. Data points are connected by straight lines. Dotted lines are the same as those straight lines in Fig. 4 A. (C) Averaged open durations as a function of internal Cl^- activity. Symbols are the same as in B. Dotted curves are the same as the solid curves in Fig. 4 B. Note that in the presence of E127Q mutation, the mutation effects from varying the charge at position 519 were nearly eliminated.

residues other than K519. The locations of several pore residues, including E127, Y512, D513, I515, and K519, are shown in Fig. 1. For the single E127Q mutant, the fast gating properties are the same as those of the WT channel (see Fig. 7 of Chen and Chen, 2003). However, the functional role of this mutation on the fast gating is revealed in the concurrent mutations of E127 and K519. After removing the negative charge at position 127, the channels with either a positive, neutral, or negative charge at position 519 all have a similar open duration of the fast gate (Fig. 6 A, closed circles in dwell-time histograms). The slight differences in the duration of the closed events (open squares) among the three dwell-time histograms appear to be within a normal variation from patch to patch. Fig. 6, B and C, compare the averaged closed and open durations of the three K519 mutations in the absence and in the presence of the E127Q mutation. The closed durations (reflecting opening rate) from the three channels are ∼15–35 ms at all $[Cl^-]_i$, and the effects from charge alterations are absent whether E127Q mutation is present or not, indicating that E127Q mutation has limited influences on the fast-gate opening mechanism (Fig. 6 B). On the other hand, even though the open duration in these mutants is still controlled by internal Cl^- to the same degree as that in the WT channel, the open durations of the three K519 mutants in E127Q background are almost identical to each other, and they are also similar to those of the WT channel at various $[Cl^-]_i$ (Fig. 6 C). These results indicate that E127 residue did play an important role in regulating the closing rate of the fast gate. However, it appears that the negative charge of this residue interacts with the positive charge from the K519 side chain in an unknown manner to exert the electrostatic control on the fast-gating mechanism.

The electrostatic regulation of the fast gating in the pore was further investigated by examining more charge mutations at three positions—positions E127,

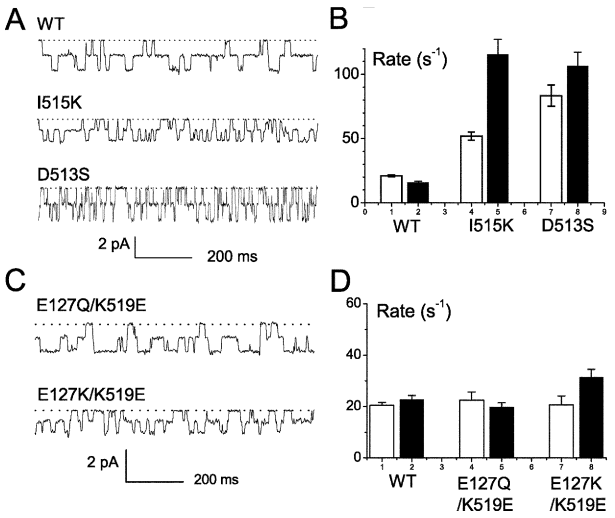

FIGURE 7. Increase of the fast-gating transition rate by increasing positive potential in the pore. (A) Single-channel recordings of WT, I515K and D513S mutants at $V_m = -90$ mV and $[Cl^-]_i = 600$ mM. Dotted lines represent zero-current level. (B) Comparison of the averaged opening (open bars) and the closing rates (filled bars) among the WT channel, I515K and D513S. V_m and $[Cl^-]_i$ are as described in A. Both the opening and closing rates of the mutants are significantly larger than those of the WT channel. (C) Placing positive charge at position 127 also speeds up the fast gating. Recording traces of the double mutants were taken at $V_m = -90$ mV and $[Cl^-]_i = 300$ mM. Note that the only structural difference of these two double mutants was the mutation at position 127. (D) Comparison of the opening (open bars) and closing rates (filled bars) of the WT channel and the double mutants involving positions 127 and 519. The opening rates among three channels are not significantly different. The closing rate of E127K/K519E is significantly larger than that of the WT channel and of the E127Q/K519E double mutant.

D513, and I515. These three residues correspond to E111, S446, and I448 of the bacterial ClC channel, respectively, and they are all deeper in the pore than position 519 (see the three dark gray residues in Fig. 1). The distances from the glutamate gate or from the central Cl^- binding site, S_{cen}, to each of the three residues appear to be roughly equal, but E127 and I515 are closer to the internal Cl^- binding site, S_{int}, than D513. The single-channel recordings of I515K and D513S are shown in Fig. 7 A. Placing a positive charge at position 515 (I515K) speeds up the fast gating. This effect can be reproduced by modifying I515C with 2-aminoethyl methanethiosulfonate (MTSEA) or 3-aminopropyl methanethiosulfonate (MTSPA) (unpublished data), each of which attaches a positive charge to the side chain of the introduced cysteine. The fast-gate opening and closing rates are also increased when the negative charge at D513 is removed. On average, adding a positive charge at position 515 (WT to I515K) increases the opening and closing rates by ~2.5- and ~7.3-fold, whereas removing a negative charge at position 513 (WT to D513S) increases the opening and closing rate by ~4.0- and ~6.7-fold, respectively (Fig. 7 B). We also replaced E127 with a positively charged residue. The single-point mutant E127K was not functionally expressed. We therefore compared the gating behavior of the double mutant E127K/K519E with that of E127Q/K519E (Fig. 7 C). Again, a more positive charge at position 127 also increases the closing rate of the channel by ~50% even though the opening rate in both mutant channels is not significantly different from that of the WT channel (Fig. 7 D). The results thus demonstrate that introducing positively charged residues (or removing negatively charged residues) in the pore consistently speeds up the fast gating of ClC-0. On the other hand, introducing negative charges in the pore (for example, K519E and I515E/E127Q mutants, or K519C modified with 2-sulfonatoethyl methanethiosulfonate (MTSES), unpublished data) makes the fast gating become slower. Thus, increasing $[Cl^-]_i$ and introducing more negative charge to the pore lead to a similar effect—an energetic stabilization of the open state of the fast gate.

The above charge mutations could influence the fast gating via a direct, through-space, electrostatic interaction with the negatively charged E166 side chain or the effects could be mediated by the permeant ions in the pore, a mechanism that might underlie the gating-permeation coupling. To explore this latter possibility, we examined whether the fast-gating properties could be altered by mutations which alter the channel conductance without charge alteration. The two mutations S123T and Y512F both changed the conductance of ClC-0 significantly (Chen and Chen, 2003). The conductance of the mutant S123T was consistently small throughout the whole range of $[Cl^-]_i$, and the duration of the open events appeared longer than the WT channel as judged from the single-channel traces (Fig. 8 A, lower traces). The small conductance of this mutant, however, prevents an accurate evaluation of the gating parameters. Consequently, we only focused on the analysis of the gating parameters of the Y512F mutant. The durations of the fully open events of the fast gate of Y512F appear to be longer than those of the WT channel at both 300 and 2,400 mM $[Cl^-]_i$ (Fig. 8 A, middle traces). Fig. 8, B and C, compare the averaged closed (τ_c, the inverse of the opening rate) and open durations (τ_o, the inverse of the closing rate) of Y512F with those of the charged mutants at position 519. It is apparent that for all of these channels, varying $[Cl^-]_i$ significantly changes the τ_o (or the closing rate) but not τ_c (opening rate). The τ_o of the Y512F mutant approaches that of the WT channel at low $[Cl^-]_i$. At high $[Cl^-]_i$, however, the τ_o of the Y512F mutant becomes even longer than that of the K519E mutant. Curve fitting for the data points reveals that the saturated open duration

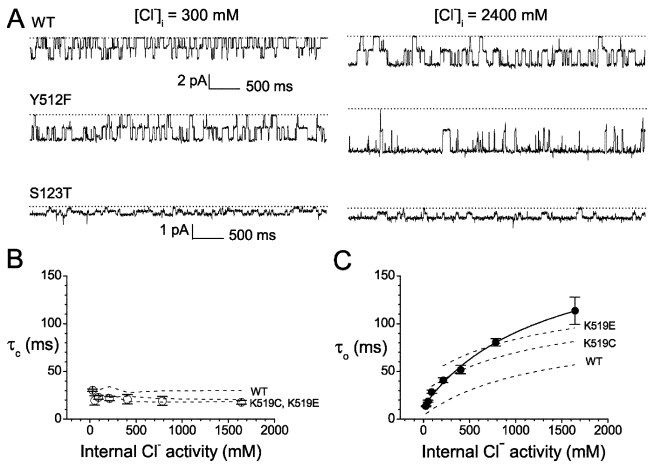

FIGURE 8. Internal Cl^- titration on the closed (τ_c) and the open durations (τ_o) of the mutants at the selectivity filter. (A) Single-channel recording traces for the mutants Y512F and S123T at 300 and 2400 mM $[Cl^-]_i$. $V_m = -110$ mV. For comparison, the traces of the WT channel at the same recording conditions are also shown. The vertical scale for the S123T traces (left and right) is expanded to better show the close-open transition of this channel. (B) Effects of raising $[Cl^-]_i$ on τ_c of Y512F. Data points were calculated from opening rate at –110 mV according to Eq. 3b. The values of τ_c for WT, K519C and K519E connected by dotted lines are the same as those in Fig. 4 A. Those values for Y512F are shown as open circles. (C) Effects of raising $[Cl^-]_i$ on τ_o. Data at -110 mV were used to calculate τ_o according to Eq. 3a. Closed circles represent the values for Y512F. Dotted curves were taken from Fig. 4 B. The solid curve was drawn according to a curve fitting to Eq. 4, with the fitted parameters of 12.9 ms, 182.1 ms, and 1334.9 mM for τ_{min}, τ_{max}, and $K_{1/2}$, respectively.

of the Y512F mutant is approximately twofold longer than that of the WT channel. The apparent affinity of Cl^- in mediating the effect, however, is roughly similar to that of the WT channel. Thus, the mutation Y512F does not change the opening rate of the fast gate, but alters the range of the fast-gate closing rate that is controlled by $[Cl^-]_i$.

DISCUSSION

We have studied the internal Cl^- effects and the electrostatic regulations on the fast gating of ClC-0. An increase of $[Cl^-]_i$ significantly reduces the closing rate (or increases the open duration) of the fast-gate, but has almost no effect on the opening rate of the fast gate (except a small influence by very high $[Cl^-]_i$ at the depolarized voltages for the WT channel). This internal Cl^- regulation on the fast-gate closing rate has been observed previously, although no mechanistic explanation was offered (Chen and Miller, 1996). The analogy of "foot-in-the-door" (Chen and Miller, 1996) implies that the effect is mediated by a binding site (or binding sites) close to the channel gate. When examining the dependence of the open duration on the internal Cl^- activity, we found that the relation is not linear, but is described by a hyperbolic curve. This observation is significant because it implies that the Cl^- effect on the open duration is saturable. The fact that Br^- but not SO_4^{2-} can exert a similar gating effect (Fig. 5 B) shows that permeant ions can reach this binding site but not nonpermeant ions. Finally, the effect of Br^- in reducing the closing rate appears to be larger than that of Cl^- (Fig. 5 B). This may be due to a higher Br^--binding affinity than that of Cl^- in the pore. These results are all consistent with the idea that the Cl^- regulation on the closing rate is through specific ion-binding sites in the pore. However, the Cl^- titration curve reveals that Cl^- has a very low apparent affinity in mediating this gating effect, with a half-saturating Cl^- activity in the molar range. In comparison, the half-saturating Cl^- activity for the channel conductance is ~60–75 mM (Chen and Chen, 2003; also see White and Miller, 1981). The results from Br^- experiments also suggest that the affinity of Br^- in increasing the open duration is significantly lower than that of Br^- in reducing the channel conductance (Fig. 5). Therefore, although controls of channel gating and pore conductance are likely to be mediated by the same ion-binding sites in the pore, the contribution of each binding site to the regulation of the fast-gate closing and to the determination of the channel conductance is probably different.

In addition to the Cl^- effect on the open duration, we have found that charge mutations in the inner pore region also alter the close-open transition rate of the fast gating. Although the mutations could create unexpected conformational changes that might allosterically alter the fast gating, for several reasons we think that a major portion of the mutation effects on the fast-gate closure comes from an electrostatic mechanism. First, the effects of mutations at position 519 concur with the charge instead of the size or shape of the mutated side chain. Thus, the fast-gating of K519F or K519M is similar to that of K519C while the gating of K519D is similar to K519E (see recording traces in Fig. 8 of Chen and Chen, 2003). Second, the effect on the fast-gate closure (duration of open events) from the mutation of a positively charged residue K519 can be nearly eliminated by a simultaneous counter-charge mutation, E127Q (Fig. 6). Finally, we have consistently found that increasing the positive charge in the inner pore region increases the open-close transition rate of the fast gate (Fig. 7). The effect is most notable when charge manipulations occurred at I515 and D513. Although the effect is less prominent at position 127, we suspect that this is likely due to the fact that E127 may interact with K519, and therefore its negativity is reduced by the nearby positive charge from K519. Likewise, when the double mutant E127K/K519E was

made, the positive potential of E127K was reduced by the negative charge of the K519E side chain. However, comparing the E127K/K519E mutant with the E127Q/K519E mutant still shows that the former double mutant has a faster closing rate than the latter (Fig. 7, C and D). Therefore, the results from charge mutations at position 127 and 519 are also consistent with those results obtained at positions 515 and 513—a more positive potential in the pore results in a faster fast gating.

The observation that changing $[Cl^-]_i$ and altering electrostatic potential in the pore both affect the fast gating in a similar manner—for example, influence the closing rate more than the opening rate, and shift the closing rate curve in parallel—suggests that these two different manipulations may act through similar mechanisms. What are the possible mechanisms underlying these effects? The crystal structures of the bacterial ClC channels reveal that the side chain of E148 occludes the ion permeation pathway, suggesting that the side chain of the corresponding glutamate (E166) in ClC-0 might be the gate (Dutzler et al., 2002). The structures of the E148 mutants of the bacterial channel further show that the pore contains an uninterrupted queue of three Cl^- ions in the pore (Dutzler et al., 2003). In particular, one of the Cl^- ions binds to the external Cl^- binding site, S_{ext}, in place of the negatively charged side chain of E148 in the wild-type bacterial channel. This structural picture suggests that Cl^- may occupy S_{ext} position to compete with the negatively charged side chain of E166 of ClC-0, and thus prevent the E166 side chain from adopting a closed position (Dutzler et al., 2003). Such a competition mechanism, therefore, almost perfectly explains the "foot-in-the-door" effect exerted by the internal Cl^-.

Under the assumption that E166 of ClC-0 is the fast gate, we considered two possibilities for how the charge mutations at the inner pore region could influence the fast gating. First, the negative charge on the gate could directly interact, via a through-space electrostatic force, with the charged residues in the inner pore region. A more negative potential from the inner pore region would repel the gate so that it is more difficult to close. Although some of the charge mutations shown above are fairly distant from the side chain of E166—for example, the charge on the side chains of E127 and K519 are ~15 and 20 Å away from the side chain of E166, respectively—the dielectric constant within protein molecules is usually much smaller than that in the bulk water solution. A direct electrostatic influence on the glutamate gate, however, cannot completely explain all the phenomena. For example, the WT channel (E127/K519) and the E127K/K519E double mutant have their positive and negative charges swapped at positions 127 and 519, but the charge pair is preserved. However, the fast-gate closing rate was increased by ~50% in the double mutant (Fig. 7 D). One may argue that since position 127 is deeper in the pore than position 519, it is closer to the negatively charged residue E166. Consequently, E127K/K519E channel would exert a more positive potential toward the glutamate gate, leading to a faster gating mechanism. However, if a positive charge at position 127 can have an electrostatic influence on the glutamate gate, why would a removal of the negative charge at this position (E127Q) have little effect on the fast-gate closure?

A second possibility to explain the effect of charge mutation on the fast gating would invoke a mediating role for the permeant ion. Mutation of E127Q by itself has no effect on the gating. However, this mutation nearly removes the mutational effects of K519 on the closing rate. Although the nature of the asymmetric effects from the mutations of these two neighboring residues is unknown, the influence on gating by the E127Q mutation mirrors the effect of this mutation on channel conductance (Chen and Chen, 2003). Such a similarity argues that the mutational effect on the fast gating could be partly mediated by permeant ions. For example, the charge effect on the fast gating may involve the electrostatic force in the pore from the Cl^- at S_{int} to that at S_{ext}. The pore conductance is controlled by the charge placed at positions 127, 515, and 519, which are located on the intracellular side of S_{int} (Chen and Chen, 2003). When more positive charges are placed at these positions, the potential for Cl^- at S_{int} to repel the Cl^- at S_{cen} and then the one at S_{ext} would be decreased. This would decrease the competition of Cl^- for S_{ext} with the side chain of E166. Consequently, the E166 side chain may more easily assume its closed position—a faster closing rate of the fast gate.

Although this ion–ion interaction mechanism qualitatively explains the electrostatic control on the fast gating, a quantitative comparison between the effects on pore conductance and fast gating is not completely satisfactory. For example, the E127K/K519E double mutant has a similar conductance-Cl^- activity curve as that of the I515K mutant (Fig. 9 in Chen and Chen, 2003). However, the fast gating of the latter is much faster than the former. Similarly, the D513S and I515K mutants have a similar closing rate, but their conductances are quite different (Fig. 7, A and B). We suspect that there is a position effect, and depending on the location where the charge is manipulated, the above two mechanisms may have different contributions. At positions more distant from the permeation pathway (for example D513), a through-space electrostatic effect may be more important. On the other hand, at positions closer to permeant ions, like E127 and K519, the electrostatic effect mediated by the permeant ions may be more prominent. Since the electrostatic potential in the pore is altered by ion binding (Miller, 1999; Non-

ner et al., 1999; also see Lin and Chen, 2003), it is likely that the internal Cl^- controls on the closing rate are also a combination of the above two effects—that is, a direct competition of Cl^- with the E166 side chain and the overall more negative potential brought to the pore by Cl^- binding. These two mechanisms, however, are probably not separable even though we have intentionally discussed them individually.

Besides an effect on the closing rate of the fast gate, some mutants presented in this study (for example, I515K or D513S) also alter the fast-gate opening rate. Simultaneous increases of the opening and the closing rate by a point mutation could result from a reduction of the transition state energy in a reversible gating process. However, several observations suggest that the fast-gate opening and closing of ClC-0, at the microscopic level, might not be the reverse process of one another. First, the opening and the closing mechanisms are regulated differently by external and internal Cl^-. Second, each mutation we have created has a different magnitude effect on the opening and the closing rate. In the present study, in which internal manipulations (such as alterations of $[Cl^-]_i$ and mutations of residues intracellular to the glutamate gate) are made, changes in the closing rate are always larger than those in the opening rate. On the other hand, extracellular manipulations—for example, alterations of $[Cl^-]_o$ (Chen and Miller, 1996) and the modification of K165C by MTSEA (Lin and Chen, 2000)—mainly change the opening rate. Finally, the apparent affinity for external Cl^- to regulate the opening rate is ~50 mM (Chen and Miller, 1996), while the affinity for the internal Cl^- to regulate the closing rate is ~1.3 M (Fig. 4). These observations together may suggest that protein conformational changes involved in the opening and closing of the fast gate are not the reverse of each other, a possibility consistent with the essence of the nonequilibrium gating cycle proposed previously (Richard and Miller, 1990).

Thus, the functions of the fast gate appear to be more complicated than the very simple form of local motions of an amino acid sidechain as envisioned from the crystal structures of the bacterial ClC channels shown in Dutzler et al. (2003). The competition of Cl^- with the negatively charged E166 sidechain may account for the internal Cl^- effect on the closing rate, but it is difficult to explain the external Cl^- effect on the opening rate. Because the apparent Cl^- affinities for external and internal Cl^- to control the fast gating are very different, it is unlikely that external Cl^- would modulate the opening rate by directly binding to the S_{ext} site, which appears to have an intimate relation with the internal Cl^- control of the closing rate. If this is the case, the Cl^- binding site for the external Cl^--dependent, depolarization-favored, opening of the fast gate should not correspond to any of the three Cl^--binding sites revealed in the most recent crystal structure of the *E. coli* ClC channel (Chen, 2003). It would be interesting to explore the structural basis of the fast-gate opening by extracellular Cl^- ions. In these future studies, however, separating the opening from the closing process of the fast gating would be important in order to properly address the irreversible nature of the gating in ClC-0.

We are grateful to Dr. R.H. Fairclough and Dr. T.-C. Hwang for their constant advice during the whole course of the study. We also thank Dr. R. MacKinnon for sharing the crystal structures of the E148 mutants of the *E. coli* ClC channels prior to publication.

This work was supported by a Health Science Research Award from UC Davis and a National Institutes of Health grant GM65447.

Olaf S. Andersen served as editor.

Submitted: 7 April 2003
Accepted: 3 October 2003

REFERENCES

Bauer, C.K., K. Steinmeyer, J.R. Schwarz, and T.J. Jentsch. 1991. Completely functional double-barreled chloride channel expressed from a single *Torpedo* cDNA. *Proc. Natl. Acad. Sci. USA.* 88: 11052–11056.

Chen, M.-F., and T.-Y. Chen. 2001. Different fast-gate regulation by external Cl^- and H^+ of the muscle-type ClC chloride channel. *J. Gen. Physiol.* 118:23–32.

Chen, M.-F., and T.-Y. Chen. 2003. Side-chain charge effects and conductance determinants in the pore of ClC-0 chloride channel. *J. Gen. Physiol.* 122:133–145.

Chen, T.-Y. 1998. Extracellular zinc ion inhibits ClC-0 chloride channels by facilitating slow gating. *J. Gen. Physiol.* 112:715–726.

Chen, T.-Y. 2003. Coupling gating with ion permeation in ClC channels. *Sci. STKE* 2003: pe23.

Chen, T.-Y., and C. Miller. 1996. Nonequilibrium gating and voltage dependence of the ClC-0 Cl^- channel. *J. Gen. Physiol.* 108:237–250.

Dutzler, R., E.B. Campbell, M. Cadene, B.T. Chait, and R. MacKinnon. 2002. X-ray structure of a ClC chloride channel at 3.0 Å reveals the molecular basis of anion selectivity. *Nature.* 415:287–294.

Dutzler, R., E.B. Campbell, and R. MacKinnon. 2003. Gating the selectivity filter in ClC chloride channels. *Science.* 300:108–112.

Hanke, W., and C. Miller. 1983. Single chloride channels from *Torpedo* electroplax: activation by protons. *J. Gen. Physiol.* 82:25–45.

Hamill, O.P., A. Marty, E. Neher, B. Sakmann, and F.J. Sigworth. 1981. Improved patch-clamp techniques for high-resolution current recording from cells and cell-free membrane patches. *Pflugers Arch.* 391:85–100.

Jentsch, T.J., T. Friedrich, A. Schriever, and H. Yamada. 1999. The CLC chloride channel family. *Pflügers Arch.-Eur. J. Physiol.* 437: 783–795.

Jentsch, T.J., V. Stein, F. Weinreich, and A. Zdebik. 2002. Molecular structure and physiological function of chloride channels. *Physiol. Rev.* 82:503–568.

Jentsch, T.J., K. Steinmeyer, and G. Schwarz. 1990. Primary structure of *Torpedo marmorata* chloride channel isolated by expression cloning in *Xenopus* oocytes. *Nature.* 348:510–514.

Lin, C.-W., and T.-Y. Chen. 2000. Cysteine modification of a putative pore residue in ClC-0: implication for the pore stoichiometry of ClC chloride channels. *J. Gen. Physiol.* 116:535–546.

Lin, C.-W., and T.-Y. Chen. 2003. Probing the pore of ClC-0 by substituted cysteine accessibility method using methane thiosulfonate reagents. *J. Gen. Physiol.* 122:147–159.

Lin, Y.-W., C.-W. Lin, and T.-Y. Chen. 1999. Elimination of the slow gating of ClC-0 chloride channel by a point mutation. *J. Gen. Physiol.* 114:1–12.

Ludewig, U., M. Pusch, and T.J. Jentsch. 1996. Two physically distinct pores in the dimeric ClC-0 chloride channel. *Nature.* 383: 340–343.

Maduke, M., C. Miller, and J.A. Mindell. 2000. A decade of CLC chloride channels: structure, mechanism, and many unsettled questions. *Annu. Rev. Biophys. Biomol. Struct.* 29:411–438.

Middleton, R.E., D.J. Pheasant, and C. Miller. 1994. Purification, reconstitution, and subunit composition of a voltage-gated chloride channel from *Torpedo* electroplax. *Biochemistry.* 33:13189–13198.

Middleton, R.E., D.J. Pheasant, and C. Miller. 1996. Homodimeric architecture of a ClC-type chloride ion channel. *Nature.* 383:337–340.

Miller, C. 1982. Open-state substructure of single chloride channels from *Torpedo* electroplax. *Philos. Trans. R Soc. Lond. B Biol. Sci.* 299:401–411.

Miller, C. 1999. Ionic hopping defended. *J. Gen. Physiol.* 113:783–787.

Miller, C., and E.A. Richards. 1990. The *Torpedo* chloride channel: intimations of molecular structure from quirks of single-channel function. *In* Chloride Transporters. A. Leefmans and J. Russel, editors. Plenum Press, New York. 383–405.

Miller, C., and M.M. White. 1984. Dimeric structure of single chloride channels from *Torpedo* electroplax. *Proc. Natl. Acad. Sci. USA.* 81:2772–2775.

Nonner, W., D.P. Chen, and B. Eisenberg. 1999. Progress and prospects in permeation. *J. Gen. Physiol.* 113:773–782.

O'Neill, G.P., R. Grygorczyk, M. Adam, and A.W. Ford-Hutchinson. 1991. The nucleotide sequence of a voltage-gated chloride channel from the electric organ of *Torpedo californica. Biochim. Biophys. Acta.* 1129:131–134.

Pusch, M., U. Ludewig, A. Rehfeldt, and T.J. Jentsch. 1995. Gating of the voltage-dependent chloride channel ClC-0 by the permeant anion. *Nature.* 373:527–531.

Richard, E.A., and C. Miller. 1990. Steady-state coupling of ion-channel conformations to a transmembrane ion gradient. *Science.* 247:1208–1210.

Swenson, R.P., and C.M. Armstrong. 1981. K^+ channels close more slowly in the presence of external K^+ and Rb^+. *Nature.* 291:427–429.

Robinson, R.A., and R.H. Stokes. 1955. Activity coefficients of electrolytes at 25°C. *In* Electrolyte Solutions. Academic Press Inc., New York, NY. 477 pp.

White, M.M., and C. Miller. 1979. A voltage-gated anion channel from the electric organ of *Torpedo californica. J. Biol. Chem.* 254: 10161–10166.

White, M.M., and C. Miller. 1981. Probes of the conduction process of a voltage-gated Cl^- channel from *Torpedo* electroplax. *J. Gen. Physiol.* 78:1–18.